








## Article

# Synthesis, Structure, Biological Activity, and Luminescence Properties of a “Butterfly”-Type Silver Cluster with 3-Benzyl-4-phenyl-1,2,4-triazol-5-thiol

Dmitriy S. Yambulatov <sup>1,\*</sup>, Irina A. Lutsenko <sup>1</sup>, Dmitry E. Baravikov <sup>1,†</sup>, Fedor M. Dolgushin <sup>1</sup>, Tatiana V. Astaf'eva <sup>1</sup>, Olga B. Bekker <sup>2</sup>, Lusik G. Nersisyan <sup>3</sup>, Melanya A. Samvelyan <sup>3</sup>, Taniel V. Ghochikyan <sup>3</sup>, Mikhail A. Kiskin <sup>1</sup>, Igor L. Eremenko <sup>1</sup> and Vladimir K. Ivanov <sup>1</sup>

<sup>1</sup> Kurnakov Institute of General and Inorganic Chemistry, Russian Academy of Sciences, 31 Leninsky Prosp., 119991 Moscow, Russia; irinalu05@rambler.ru (I.A.L.); dbbaravikov@gmail.com (D.E.B.); fmdolgushin@gmail.com (F.M.D.); tata1525@mail.ru (T.V.A.); m\_kiskin@mail.ru (M.A.K.); ileremenko@yandex.ru (I.L.E.); van@igic.ras.ru (V.K.I.)

<sup>2</sup> Vavilov Institute of General Genetics, Russian Academy of Sciences, Gubkina, 3, 119333 Moscow, Russia; obekker@yandex.ru

<sup>3</sup> Faculty of Chemistry, Yerevan State University, 1 A Manoukian Str., Yerevan 0025, Armenia; nersisyanlusik@mail.ru (L.G.N.); msamvelyan@ysu.am (M.A.S.); tghochikyan@gmail.com (T.V.G.)

\* Correspondence: yambulatov@igic.ras.ru or yambulatov@yandex.ru; Fax: +7-(495)-955-4817

† The article is dedicated to the memory of our student, colleague, friend, real scientist Dmitry Baravikov.

**Abstract:** A new silver(I) cluster [Ag<sub>8</sub>L<sub>4</sub>(Py)(Pype)]·4Py·11H<sub>2</sub>O (**I**) with 3-benzyl-4-phenyl-1,2,4-triazol-5-thiol (**L**) was synthesized via the direct reaction of AgNO<sub>3</sub> and **L** in MeOH, followed by recrystallization from a pyridine–piperidine mixture. The compound **I** was isolated in a monocrystal form and its crystal structure was determined via single crystal X-ray diffraction. The complex forms a “butterfly” cluster with triazol-5-thioles. The purity of the silver complex and its stability in the solution was confirmed via NMR analysis. Excitation and emission of the free ligand and its silver complex were studied at room temperature for solid samples. The in vitro biological activity of the free ligand and its complex was studied in relation to the non-pathogenic *Mycolicobacterium smegmatis* strain. Complexation of the free ligand with silver increases the biological activity of the former by almost twenty times. For the newly obtained silver cluster, a bactericidal effect was established.

**Keywords:** 1,2,4-triazole; silver; molecular structure; luminescence; single crystal; metallodrugs; biological activity



**Citation:** Yambulatov, D.S.; Lutsenko, I.A.; Baravikov, D.E.; Dolgushin, F.M.; Astaf'eva, T.V.; Bekker, O.B.; Nersisyan, L.G.; Samvelyan, M.A.; Ghochikyan, T.V.; Kiskin, M.A.; et al. Synthesis, Structure, Biological Activity, and Luminescence Properties of a “Butterfly”-Type Silver Cluster with 3-Benzyl-4-phenyl-1,2,4-triazol-5-thiol. *Molecules* **2024**, *29*, 105.

<https://doi.org/10.3390/molecules29010105>

molecules29010105

Academic Editor: Xingcai Wu

Received: 6 December 2023

Revised: 17 December 2023

Accepted: 20 December 2023

Published: 23 December 2023



**Copyright:** © 2023 by the authors. Licensee MDPI, Basel, Switzerland. This article is an open access article distributed under the terms and conditions of the Creative Commons Attribution (CC BY) license (<https://creativecommons.org/licenses/by/4.0/>).

## 1. Introduction

The current approach of advanced bioinorganic chemistry consists of using simple well-known biologically active molecules to design effective metallodrugs. Such ligands include, for example, benzimidazole derivatives [1,2]; purine bases [3,4], particularly caffeine [5–9]; the well-known commercially available ligand 1,10-phenanthroline [10]; anions of biologically active carboxylic acids (benzoic [11,12], 2-furoic [13,14], etc.); dithiocarbamates [15,16]; and redox-active ligands [17–21]. In most cases, after coordination of a biologically active molecule to a metal ion, the bioactivity of the resulting complex increases significantly [22–26], simultaneously reducing the toxicity and, therefore, the lethal dose of an organic ligand, which make it possible to use this substance in therapy.

A well-studied family of biologically active ligands that can be used to create new metallodrugs includes the derivatives of 1,2,4-triazoles, which have been known for more than 100 years and the methods of their synthesis and chemical properties have been studied extensively [27]. Their biological activity has been proven via many years of clinical use as drugs registered in the European Pharmacopoeia, for example, Alprazolam (sedative), Anastrozole (treatment for breast cancer), Brotizolam (sedative), Fluconazole (antifungal),

Itraconazole (antifungal), Letrozole (treatment for breast cancer), Ribavirin (antiviral), Terconazole (antifungal), and Trapidi (antiaggregant) [28]. Despite more than a century-long history of studying triazoles, they still attract the attention of researchers [29]. When designing novel bioactive metal complexes, it is very important to know the mechanism of pharmacokinetics; in the case of 1,2,4-triazole derivatives, these data are already available [30–32], which can facilitate and reduce the cost of further testing of the corresponding metallodrugs.

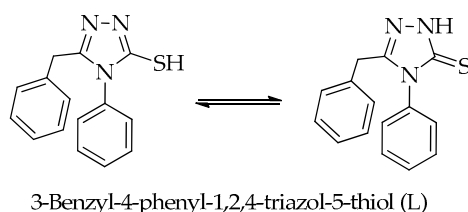
To date, reliable data have been obtained on the antifungal, antioxidant, anticonvulsant, anti-inflammatory activity of metal complexes with 1,2,4-triazoles and their potential use for the treatment of tuberculosis, diabetes, and different types of cancer [33,34]. It was shown that triazole-derived Schiff base ligands and their cobalt(II), nickel(II), copper(II), and zinc(II) complexes reveal antibacterial and antifungal activity, of which the study proved that the metal complexes showed better activity than the ligands after coordination [35,36]. It was also shown that the addition of other donor atoms (oxygen, nitrogen, and sulfur) to triazole derivatives leads to the formation of biologically active complexes. For example, vanadyl(IV) complexes with mono- and di-substituted ONS donor triazoles reveal antibacterial, antifungal, and cytotoxic activity [37,38].

According to the previous studies, silver cation is a promising complex-forming ion in the design of metallodrugs [39–42]. Silver-containing compounds are currently used for the therapy of skin diseases and burns: silver sulfadiazine [39], silver proteinate (Protargol) [43], and silver nitrate [44]. Since silver has long been used in the treatment of various diseases, its pharmacokinetics, like 1,2,4-triazole derivatives, are also well studied [45,46]. Having analyzed the Cambridge structural database, we found that only a few dozen structurally characterized silver complexes with 1,2,4-triazole derivatives are known, and to the best of our knowledge, the biological activity of these compounds have not been studied.

Bioactive luminescent metallodrugs are of great interest in the field of bioinorganic chemistry due to the potential applications of these compounds for the imaging of living cells [47]. This approach can be used to track the distribution of luminescent substances within a cell and study their uptake by cells [48]. Undoubtedly, the leaders in bioimaging among compounds used in modern medicine and biology are complexes based on lanthanides [49,50]. However, currently more and more research is devoted to promising luminescent probes in living systems based on Ag(I) (with simultaneous antibacterial properties). It was found that luminescent properties of Au(I) and Ag(I) complexes with N-heterocyclic carbenes can be used to investigate biodistribution [51].

The previously studied silver complexes with 1,2,4-triazole derivatives exhibit luminescent properties [52–54], which are very important in the design of promising metal-containing drugs [55–58]. It was also previously shown that silver has a high affinity for the sulfur atom, forming strong linear compounds or layers [59–61].

Thus, the goal of this study was to develop a method for the synthesis of a new silver complex with a 1,2,4-triazole sulfur-containing derivative—3-benzyl-4-phenyl-1,2,4-triazol-5-thiol (L, Scheme 1)—and determine its molecular structure, confirm the purity, and analyze the luminescent properties of the free ligand and the complex. Also, the purpose of this study was to find out whether the free ligand and its silver complex exhibit biological activity against *M. Smegmatis* (a model non-virulent strain of *M. tuberculosis*) and how the coordination of the ligand affects these properties. This current work is a part of our ongoing research to find new anti-tuberculosis metallodrugs [22,24–26,62].

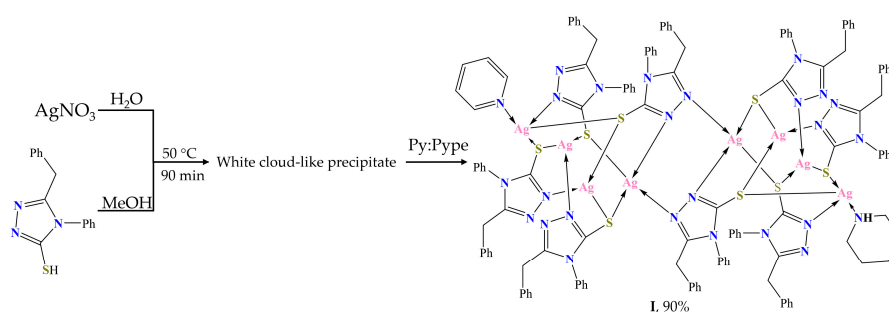


**Scheme 1.** Keto–enol tautomerization of L.

## 2. Results and Discussion

### 2.1. Synthesis and Characterization

The reaction of L and  $\text{AgNO}_3$  in a methanol solution with further crystallization from the mixture of pyridine (Py) and piperidine (Pype) (Scheme 2) led to the formation of the product  $[\text{Ag}_8\text{L}_4(\text{Py})(\text{Pype})]\cdot 4\text{Py}\cdot 11\text{H}_2\text{O}$  (I) in a form of polycrystals, suitable for single-crystal X-ray diffraction analysis. A mixture of pyridine–piperidine was used as a solvent, since similar compounds were previously obtained by adding pyridine and triphenylphosphine to a white precipitate, which indicates the need for the presence of strong bases of a donor nature to convert the resulting compound into a soluble form [63]. The reaction proceeds in air without any precautions about daylight. Decanted and twice washed with cold distilled water, the major product was isolated in a 90% yield.



**Scheme 2.** Synthesis route of compound I, solvate molecules of water and pyridine have been omitted for clarity.

The  $^1\text{H}$  NMR spectrum of I (Figure 1) is in agreement with the structural data. There is no signal of an SH proton in the  $^1\text{H}$  NMR spectrum of I, which confirms the deprotonation of the ligand. The signal of  $\text{CH}_2$  protons is upfield shifted as compared to that one for the free ligand (3.65 and 3.86 ppm, respectively—see also Supplementary Materials). The signals from CH of pyridine (7.6–9.0 ppm) and the  $\text{CH}_2$ , NH groups of piperidine (1.2–3.1 ppm) are also observed in the  $^1\text{H}$  NMR spectrum. The  $^{13}\text{C}$  NMR spectrum of I could not be recorded due to the low solubility of the compound in the common deuterated solvents. When trying to accumulate data to record a  $^{13}\text{C}$  NMR spectrum over a 24 h period, we also discovered that a white precipitate formed in the NMR ampoule. It is likely that deuterated dimethyl sulfoxide molecules replace pyridine and piperidine, reducing the solubility of complex I.

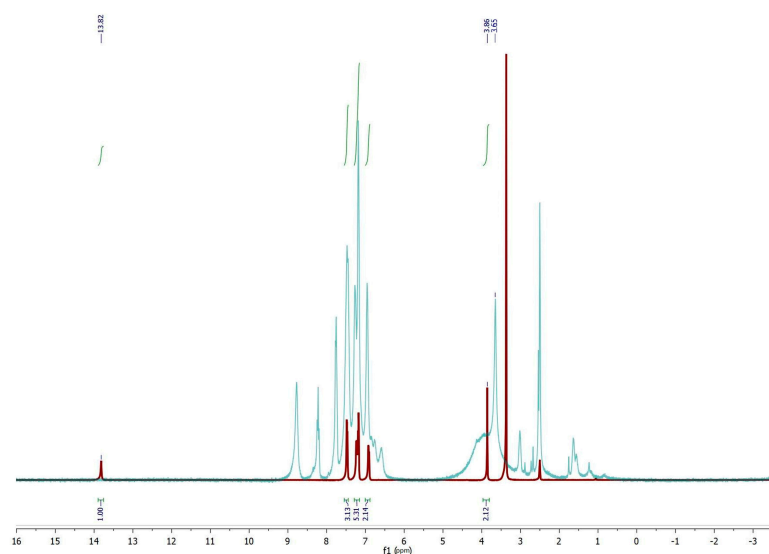


**Figure 1.**  $^1\text{H}$  NMR spectra of I (blue line) and free ligand (red line).

## 2.2. Molecular Structure of I

Complex I crystallizes in the monoclinic space group  $Pc$  in a form of crystal solvate  $[\text{Ag}_8\text{L}_4(\text{Py})(\text{Pyp})] \cdot 4\text{Py} \cdot 11\text{H}_2\text{O}$ . Since the solvate molecules of pyridine in the crystal are in strong thermal vibrations, only two solvate pyridine molecules were clearly identified, while two other molecules were taken into account as diffuse scattering using the SQUEEZE procedure [64]. Complex I is a dimer of two butterfly-type silver-metal clusters (Figures 2 and 3), in which all  $\text{Ag} \cdots \text{Ag}$  distances lie in the range of 2.969(2)–3.254(2) Å. These distances are significantly greater than the sum of the covalent 2.7 Å radii of silver and can apparently be considered as weak secondary interactions (argentophilic) [65,66].

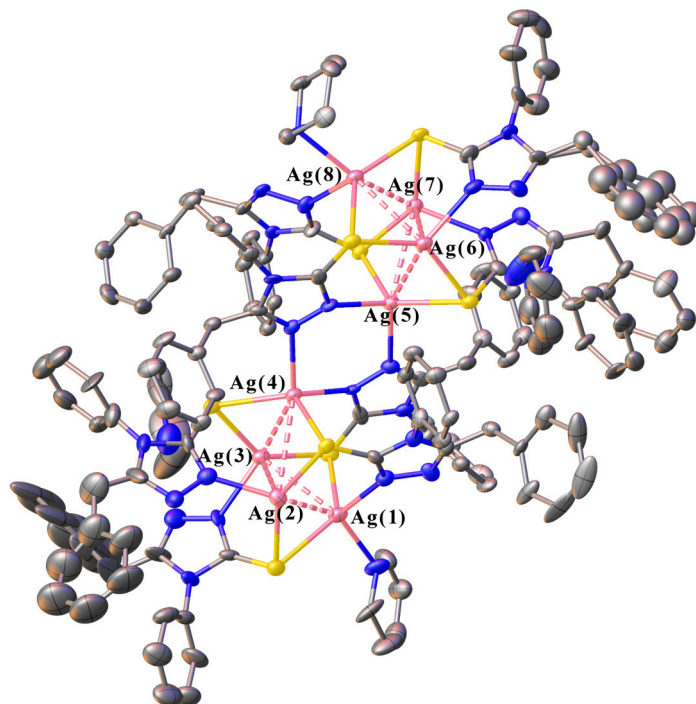


**Figure 2.** Molecular structure of I. Thermal ellipsoids are drawn at 30% probability level. Hydrogen atoms are omitted for clarity. Argentophilic interactions are shown in dotted lines.

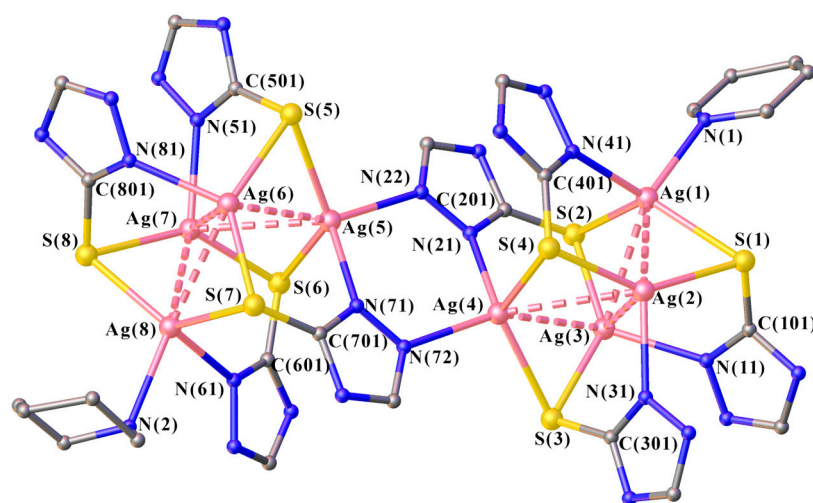


**Figure 3.** Molecular structure of I. Hydrogen atoms, solvate pyridines, and benzyl and phenyl substituents of the ligand have been omitted for clarity. Argentophilic interactions are shown in dotted lines.

Non-bonding distance between the tips of the “butterfly’s wings” ( $\text{Ag1}\cdots\text{Ag4}$  4.133(2) Å,  $\text{Ag5}\cdots\text{Ag8}$  4.236(2) Å) is significantly greater than the distance between atoms at the base of the “butterfly wings” ( $\text{Ag}\cdots\text{Ag}$  3.137(2), 3.085(2) Å). The outer vertices of the “butterfly wings” ( $\text{Ag1}$  and  $\text{Ag8}$ ) coordinate additional monodentate N-donor ligands, pyridine and piperidine, in the presence of which the synthesis and crystallization were carried out ( $\text{Ag1-N1}$  2.441(12) Å,  $\text{Ag8-N2}$  2.365(15) Å). The inner tips of the “butterfly wings” ( $\text{Ag4}$  and  $\text{Ag5}$ ) further coordinate the unsubstituted nitrogen atom in the five-membered triazol ring of one of the ligands in the adjacent butterfly to form a dimeric structure ( $\text{Ag4-N72}$  2.389(12) Å,  $\text{Ag5-N22}$  2.392(12) Å).

This molecule is pseudocentrosymmetric with the center of inversion at the center of mass of the silver atoms. The structural similarity of the two butterflies that make up the dimer is especially clearly visible when they are superimposed on each other (Figure 4). There is an almost complete coincidence of the positions of all atoms, with the exception of some differences in the orientation of the terminal benzyl substituents, as well as the difference between Py and Pype, which are coordinated by silver atoms.

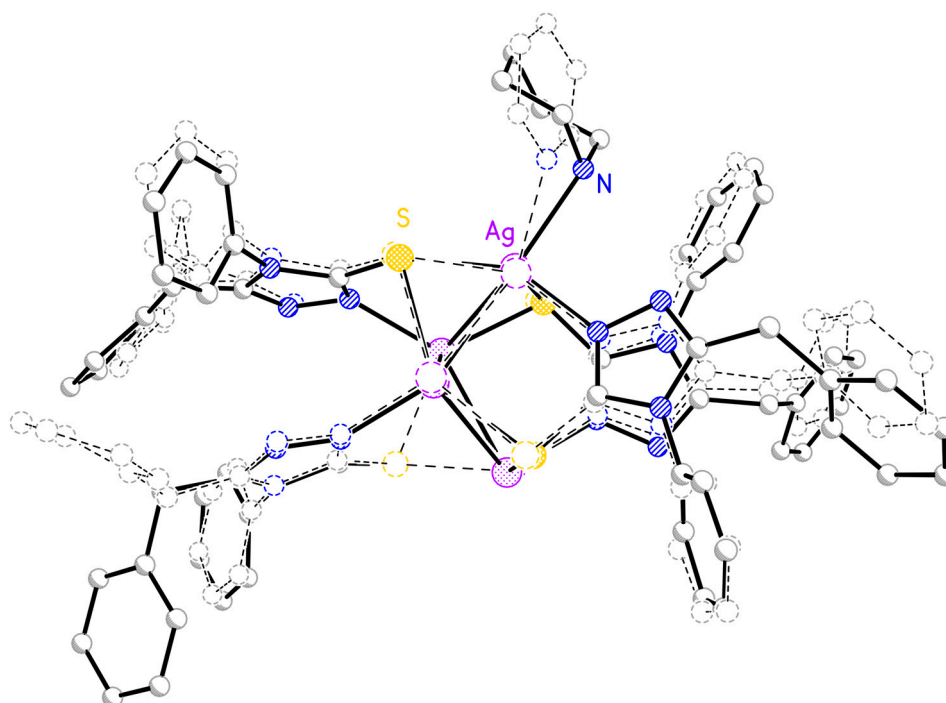


**Figure 4.** Superposition of a four-nuclear fragment of dimer I (solid line) onto another four-nuclear fragment (dashed line) via an inversion pseudocenter; the standard deviation for silver and sulfur atoms is 0.09 Å.

Four silver atoms of one part of the molecule coordinate four ligands, with each ligand bonded to three metal atoms: the nitrogen atom is bonded to one metal atom ( $\text{Ag-N}$  2.275(13)–2.358(15) Å), and a sulfur atom connects two other metal atoms ( $\text{Ag-S}$  2.421(4)–2.670(4) Å). The silver atoms at the base of the butterfly have a planar trigonal coordination  $\text{AgNS}_2$  ( $\text{CN} = 3$ ), which is typical for silver clusters formed by a ligand containing an SCN fragment, where the sulfur atom is exocyclic and the CN is endocyclic, while the silver atoms at the tops of the butterfly wings, due to an additional coordination with the N-donor fragments, have a tetrahedral coordination  $\text{AgN}_2\text{S}_2$  ( $\text{CN} = 4$ ). “Butterfly” clusters are not typical for silver with this type of ligands, and in CCDC, there is only one similar structure obtained by Robert P. Lattimer et al. [63]. Much more often a six-nuclei “Cyclohexane-Chair”-type cluster is formed [67,68].

### 2.3. Luminescent Properties

To the best of our knowledge, the luminescent properties of known silver(I) complexes have been studied mainly for square-planar polyhedrals [69], while the studied **I** contains two types of  $\text{Ag}^+$  cations with different environments—triangular and distorted tetrahedral.

The excitation spectrum of solid ligand **L** at room temperature at  $\lambda_{\text{em}} = 490$  and 510 nm gives a set of bands of 200–430 nm with a maxima at 238, 253, 281, and 400 nm, respectively (Figure S6a). In the emission spectra at  $\lambda_{\text{ex}} = 240, 250$  and 280 nm, a set of bands is observed in the region of 350–650 nm (Figure S6a), where the most intense bands have a maxima at 491, 509, and 530 nm. The excitation spectrum ( $\lambda_{\text{em}} = 400$  nm) of **I** under similar conditions is represented by broad bands in the region of 200–350 nm with a maxima at 240, 255, and 335 nm (Figure S6b). The emission spectrum of **I** at  $\lambda_{\text{ex}} = 255$  nm contains wide bands in the region of 300–600 nm with a maxima at 405, 422, and 487 nm. An analysis of the photophysical properties showed that the transition from ligand **L** to complex **I** is accompanied by a change in emission as a result of coordination of the ligand to the metal and/or transition to the anionic form. The relative emission intensity of the ligand, as well as its complex, is low.

### 2.4. Biological Activity

The biological activity of **L** and **I** was studied using the nonpathogenic mycobacterial strain *Mycobacterium smegmatis*. In mycobacterial strains, the resistance to chemical treatment agents is attributed to the low permeability of its cell wall due to its unusual structure. *M. smegmatis* is a rapidly growing nonpathogenic bacterium, which is therefore used as a model for slowly growing *Mycobacterium tuberculosis* and for the screening of antituberculosis drugs [70]. The *M. smegmatis* test system exhibits higher resistance to antibiotics and antituberculosis agents than *M. tuberculosis*; therefore, the concentration <100 nmol/disc in contrast to *M. tuberculosis* (<4  $\mu\text{g}/\text{mL}$ ) is used as the selection criterion [71]. All the results obtained for the in vitro biological activity of the compounds under study were compared with the activity of the first-line antituberculosis drug, Rifampicin (**Rif**), under the selected conditions of the experiment. The results of the antimycobacterial activity study are presented in Table 1.

**Table 1.** The results of antibacterial activity study of free ligand **L** and complex **I** against *M. smegmatis*.

Compound	MIC, (nmol/disc)	Zone of Inhibition, mm	
	24 h	24 h	120 h
<b>L</b>	>1000	0	0
<b>I</b>	50	6.5 ± 0.1	6.4 ± 0 *
$[\text{Ag}_3(\text{fur})(\text{bpy})_3]_n$ [62]	15	6.4 ± 0.12	6.2 ± 0 **
<b>Rif</b>	5	7.1 ± 0.76	7.0 ± 0.4 *

The diameter of the paper disk is 6 mm. \* The *M. smegmatis* growth inhibition zone is transparent, there is no weak background growth of the culture (bactericidal effect). \*\* *M. smegmatis* growth inhibition zone overgrows (bacteriostatic effect). 0—no growth inhibition zone.

The data shown in Table 1 demonstrate that ligand **L** does not exhibit significant biological activity against the strain of mycobacterium. In turn, the efficiency of complex **I** is increased by almost twenty times in comparison with the free ligand. Similar effect—an increase in biological activity after complex formation is observed quite often [62,72]. The effectiveness of strain suppression—like the reference drug **Rif**, **I**—has a bactericidal effect; unlike the previously obtained silver complex [62], it exhibits a bacteriostatic effect (most likely associated with the development of resistance genes of mycobacterium).

### 3. Materials and Methods

#### 3.1. General Remarks

The synthesized product **I** is stable to oxygen, moisture, and ambient light. Ligand **L** (3-benzyl-4-phenyl-1,2,4-triazol-5-thiol) was synthesized using the procedure similar to that reported earlier [73], of which its  $^1\text{H}$  and  $^{13}\text{C}$  NMR spectra (see Supplementary Information) are in good agreement with those reported previously.  $^1\text{H}$  NMR (300 MHz,  $\text{DMSO-}d_6$ )  $\delta$ : 3.86 (s, 2H,  $\text{CH}_2$ ), 6.86–6.99 (m, 2H,  $\text{C}_{\text{ar}}\text{H}$ ), 7.14–7.28 (m, 5H,  $\text{C}_{\text{ar}}\text{H}$ ), 7.42–7.55 (m, 3H,  $\text{C}_{\text{ar}}\text{H}$ ), and 13.82 (broad s, 1H, SH).  $^{13}\text{C}$  NMR (75 MHz,  $\text{DMSO-}d_6$ )  $\delta$ : 31.43, 126.86, 128.29, 128.35, 128.61, 129.27, 129.42, 133.55, 134.54, 151.27, and 167.92.

The IR spectrum of **I** was recorded in the range of 400–4000  $\text{cm}^{-1}$  using a PerkinElmer (Waltham, MA, USA) Spectrum 65 spectrophotometer equipped with a Quest ATR Accessory (Specac (Orpington, Kent, UK)). The method of attenuated total reflection (ATR) was used. Excitation and emission spectra of the solid samples were recorded at room temperature in the visible range of the spectrum using a PerkinElmer LS-55 spectrometer.

The  $^1\text{H}$  NMR spectra was registered on a Bruker AVANCE (300 MHz) spectrometer with TMS as the internal reference and  $\text{DMSO-}d_6$  as the solvent.

To study the biological activity of the free ligand **L** and its complex **I**, the paper disk method was employed using the nonpathogenic *M. smegmatis mc<sup>2</sup> 155* strain. A solution of each substance was prepared as follows: a sample of the substance was dissolved in dimethyl sulfoxide to a concentration of 100 mmol or less, depending on the solubility of the substance. Then, tenfold and twofold dilutions of the resulting solution were made and applied to paper disks in an amount of 5  $\mu\text{L}$ /disk. The test method involved measuring the size of the inhibition zone around paper discs containing a compound, which were placed on an agar plate and then seeded with the strain. The concentration of the compound was varied to determine its effect on the growth of the strain. The bacteria washed off Petri dishes with the Trypton-soy agar M-290 medium (Himedia, Mumbai, India) were grown overnight in the Lemco-TW liquid medium (Lab Lemco' Powder 5  $\text{g}\cdot\text{L}^{-1}$  (Oxoid, Basingstoke, UK), Peptone special 5  $\text{g}\cdot\text{L}^{-1}$  (Oxoid), NaCl 5  $\text{g}\cdot\text{L}^{-1}$ , Tween-80) at +37 °C until the average logarithmic growth phase occurred at optical density  $\text{OD}_{600} = 1.5$ , which was then mixed with a molten agar medium M-290 in a ratio of 1:9:10 (culture:Lemco-TW:M-290). The mixture was poured into Petri dishes containing pre-solidified agar medium (M-290) at a concentration of 5 mL/dish. After the top layer of agar had solidified, paper discs impregnated with a solution containing the test compound were placed on top of the plate. The culture was incubated for 24 h at +37 °C. The inhibition zone diameters of *M. smegmatis mc<sup>2</sup> 155* growth around the paper disks contained the free ligand **L** and its complex **I** were determined. The Minimum Inhibiting Concentration (MIC) was equal to the concentration of **L** and **I** that provided the smallest growth inhibition zone.

X-ray diffraction data for **I** were collected at 150 K with a Bruker Quest D8 CMOS diffractometer, using graphite monochromated Mo- $\text{K}\alpha$  radiation ( $\lambda = 0.71073 \text{ \AA}$ ,  $\omega$ -scans). The crystal structure of **I** was solved using Intrinsic Phasing with the ShelXT [74] in Olex2 [75] and then refined with the ShelXL [76] refinement package using Least-Squares minimization against  $F^2$  in the anisotropic approximation for non-hydrogen atoms. Hydrogen atoms were calculated and they all were refined in the isotropic approximation within the riding model. The contribution of highly disordered solvent molecules in structural voids was treated as diffuse using the SQUEEZE procedure implemented in the PLATON software, version 2023.1 [64]. The electron count within cavities ( $V_1 = 726 \text{ \AA}^3$  and  $V_2 = 688 \text{ \AA}^3$ ) measured 170 and 223  $e^-$ , respectively; per formula unit of **I**, their sum corresponds to 11 water and 4 pyridine molecules. The crystal data and structure refinement parameters are given in Table 2. CCDC 2300382 contains the supplementary crystallographic data for this manuscript.

**Table 2.** Crystal data and structure refinement for **I**.

Parameter	Value
Empirical formula	C <sub>150</sub> H <sub>154</sub> N <sub>30</sub> O <sub>11</sub> S <sub>8</sub> Ag <sub>8</sub>
Formula weight	3316.2
Crystal system	Monoclinic
Space group	<i>Pc</i>
<i>Z</i>	2
<i>T</i> , <i>K</i>	150
<i>a</i> (Å)	23.729(3)
<i>b</i> (Å)	25.401(3)
<i>c</i> (Å)	12.617(1)
$\alpha$ (°)	90
$\beta$ (°)	93.340(4)
$\gamma$ (°)	90
<i>V</i> (Å <sup>3</sup> )	7591.9(14)
<i>D</i> <sub>calc</sub> (g/cm <sup>3</sup> )	1.451
$\mu$ (Mo-K $\alpha$ ) (mm <sup>-1</sup> )	1.17
<i>F</i> (000)	3324
2 $\theta$ <sub>max</sub> (deg.)	50
<i>R</i> <sub>int</sub>	0.0988
Reflections measured	137,347
Independent reflections	118,888
Observed reflections [ <i>I</i> > 2 $\sigma$ ( <i>I</i> )]	18,266
Parameters/restraints	1447/305
<i>R</i> <sub>1</sub>	0.0561
<i>wR</i> <sub>2</sub>	0.1470
<i>Goof</i>	1.002
<i>Flack</i>	0.18(4)
$\Delta\rho_{\max}/\Delta\rho_{\min}$ (e/Å <sup>-3</sup> )	1.34/−0.96

### 3.2. Synthesis of **I**

A portion of AgNO<sub>3</sub> (0.170 g, 1 mmol) was dissolved in 5 mL of distilled water and then the solution of ligand **L** (0.270 g, 1 mmol) dissolved in 20 mL of MeOH was added, of which the resulting reaction mixture was heated at 50 °C with constant stirring and the solution gradually began to become white. After half an hour, the reaction mixture was filtered and the resulting white precipitate was dried and then redissolved in 20 mL of a 1:1 pyridine–piperidine mixture; within a week, crystals amenable for single-crystal X-ray diffraction were obtained via slow evaporation in a glass beaker capped with dotted Parafilm. The yield of the reaction is 90%. ATR-IR,  $\nu/\text{cm}^{-1}$ : 3434 w, 3057 w, 3032 w, 2919 w, 2847 w, 1631 w, 1593 w, 1524 m, 1496 m, 1424 m, 1367 s, 1311 s, 1245 s, 1160 m, 1069 m, 1031 m, 1009 m, 921 w, 824 w, 758 s, 729 s, 689 vs, 604 m, 557 s, 500 w, 465 w, 418 w, 403 w. <sup>1</sup>H NMR (300 MHz, DMSO-*d*<sub>6</sub>)  $\delta$ : 3.65 (broad s, 16H, CH<sub>2</sub>), 6.47–7.64 (m, 80H, C<sub>ar</sub>H), 7.66–7.90 (m, 8H, C<sub>py</sub>H), 8.14–8.34 (m, 4H, C<sub>py</sub>H), 8.63–8.99 (m, 8H, C<sub>py</sub>H).

### 4. Conclusions

Here, we have presented a method for preparing a new silver(I) complex with 3-benzyl-4-phenyl-1,2,4-triazol-5-thiol and determined its crystal structure. Photophysical studies of **L** and its complex **I** showed weak emission of the organic ligand in neutral and anionic form; the complexation is accompanied by the changes in the emission spectra. The study of the biological activity of **L** and **I** have determined that the free ligand does not exhibit significant bactericidal action against *Mycobacteria smegmatis*, whilst complexation with silver has increased the biological activity of the ligand by 20 times. We believe that our results may encourage chemists to synthesize novel bioactive silver complexes of 1,2,4-triazole derivatives via a facile method in water–methanol mixtures to prepare advanced pharmaceutical products.



**Supplementary Materials:** The following supporting information can be downloaded at <https://www.mdpi.com/article/10.3390/molecules29010105/s1>: Figure S1: IR-spectrum of L; Figure S2: IR-spectrum of compound I; Figure S3: IR-spectrum of L and compound I; Figure S4:  $^1\text{H}$  NMR spectrum of L; Figure S5:  $^{13}\text{C}$  NMR spectrum of L; Figure S6: Excitation and emission spectra for solid samples L (a) and I (b) at room temperature.

**Author Contributions:** Design of the study, D.S.Y., I.A.L., T.V.G., D.E.B. and M.A.S., who also synthesized the tested compounds; manuscript writing and review and editing, D.S.Y., M.A.K., T.V.G. and V.K.I.; X-ray analysis, F.M.D. and D.E.B.; funding acquisition, I.L.E., V.K.I. and L.G.N.; NMR spectroscopy, T.V.A.; biological investigation, O.B.B. and I.A.L. All authors have read and agreed to the published version of the manuscript.

**Funding:** The work was supported by the Ministry of Science and Higher Education of Russia as part of the state assignment of Kurnakov Institute of General and Inorganic Chemistry of the Russian Academy of Sciences.

**Data Availability Statement:** The structure parameters of the obtained compound were deposited with the Cambridge Structural Database (CCDC No. 2300382 (I) deposit@ccdc.cam.ac.uk or [http://www.ccdc.cam.ac.uk/data\\_request/cif](http://www.ccdc.cam.ac.uk/data_request/cif)).

**Acknowledgments:** This research was performed using the equipment of the JRC PMR IGIC RAS, supported by the state assignment of the Kurnakov Institute of General and Inorganic Chemistry, Russian Academy of Sciences, in the field of fundamental research. This work was carried out within the framework of an agreement on scientific and technological cooperation between Yerevan State University and Kurnakov Institute of General and Inorganic Chemistry of the Russian Academy of Sciences (IGIC RAS).

**Conflicts of Interest:** The authors declare no conflict of interest. The funders had no role in the design of the study; in the collection, analyses, or interpretation of the data; in the writing of the manuscript; or in the decision to publish the results.

## References

- Hernández-Romero, D.; Rosete-Luna, S.; López-Monteon, A.; Chávez-Piña, A.; Pérez-Hernández, N.; Marroquín-Flores, J.; Cruz-Navarro, A.; Pesado-Gómez, G.; Morales-Morales, D.; Colorado-Peralta, R. First-Row Transition Metal Compounds Containing Benzimidazole Ligands: An Overview of Their Anticancer and Antitumor Activity. *Coord. Chem. Rev.* **2021**, *439*, 213930. [[CrossRef](#)]
- Suárez-Moreno, G.V.; Hernández-Romero, D.; García-Barradas, Ó.; Vázquez-Vera, Ó.; Rosete-Luna, S.; Cruz-Cruz, C.A.; López-Monteon, A.; Carrillo-Ahumada, J.; Morales-Morales, D.; Colorado-Peralta, R. Second and Third-Row Transition Metal Compounds Containing Benzimidazole Ligands: An Overview of Their Anticancer and Antitumour Activity. *Coord. Chem. Rev.* **2022**, *472*, 214790. [[CrossRef](#)]
- Bland, B.R.A.; Gilfoy, H.J.; Vamvounis, G.; Robertson, K.N.; Cameron, T.S.; Aquino, M.A.S. Hydrogen Bonding in Diruthenium(II,III) Tetraacetate Complexes with Biologically Relevant Axial Ligands. *Inorg. Chim. Acta* **2005**, *358*, 3927–3936. [[CrossRef](#)]
- Melník, M.; Sprusansky, O.; Musil, P. Bio-Medical Aspects of Purine Alkaloids. *Adv. Biol. Chem.* **2014**, *4*, 274–280. [[CrossRef](#)]
- Rukk, N.S.; Kuz'mina, L.G.; Davydova, G.A.; Buzanov, G.A.; Retivov, V.M.; Belus, S.K.; Kozhukhova, E.I.; Barmashov, A.E.; Khrulev, A.A.; Simonova, M.A.; et al. Synthesis, Structure and Cytotoxicity of a Zinc(II) Bromide Complex with Caffeine. *Mendeleev Commun.* **2019**, *29*, 640–642. [[CrossRef](#)]
- Trommschläger, A.; Chotard, F.; Bertrand, B.; Amor, S.; Richard, P.; Bettaieb, A.; Paul, C.; Connat, J.-L.; Le Gendre, P.; Bodio, E. Gold(I)–Coumarin–Caffeine-Based Complexes as New Potential Anti-Inflammatory and Anticancer Trackable Agents. *ChemMedChem* **2018**, *13*, 2408–2414. [[CrossRef](#)]
- Ma, Z.; Moulton, B. Supramolecular Medicinal Chemistry: Mixed-Ligand Coordination Complexes. *Mol. Pharm.* **2007**, *4*, 373–385. [[CrossRef](#)]
- Rukk, N.S.; Kuzmina, L.G.; Shamsiev, R.S.; Davydova, G.A.; Mironova, E.A.; Ermakov, A.M.; Buzanov, G.A.; Skryabina, A.Y.; Streletskii, A.N.; Vorob'eva, G.A.; et al. Zinc(II) and Cadmium(II) Halide Complexes with Caffeine: Synthesis, X-Ray Crystal Structure, Cytotoxicity and Genotoxicity Studies. *Inorg. Chim. Acta* **2019**, *487*, 184–200. [[CrossRef](#)]
- Preedy, V.R. *Caffeine Chemistry, Analysis, Function and Effects*; The Royal Society of Chemistry: London, UK, 2012; ISBN 978-1-84973-367-0.
- Viganor, L.; Howe, O.; McCarron, P.; McCann, M.; Devereux, M. The Antibacterial Activity of Metal Complexes Containing 1, 10-Phenanthroline: Potential as Alternative Therapeutics in the Era of Antibiotic Resistance. *Curr. Top. Med. Chem.* **2017**, *17*, 1280–1302. [[CrossRef](#)]
- Nikolić, M.A.; Szécsényi, K.M.; Dražić, B.; Rodić, M.V.; Stanić, V.; Tanasković, S. Binuclear Co(II) Complexes with Macrocyclic and Carboxylate Ligands: Structure, Cytotoxicity and Thermal Behavior. *J. Mol. Struct.* **2021**, *1236*, 130133. [[CrossRef](#)]

12. Olmo, A.; Calzada, J.; Nuñez, M. Benzoic Acid and Its Derivatives as Naturally Occurring Compounds in Foods and as Additives: Uses, Exposure, and Controversy. *Crit. Rev. Food Sci. Nutr.* **2017**, *57*, 3084–3103. [[CrossRef](#)] [[PubMed](#)]
13. Melnic, S.; Prodius, D.; Simmons, C.; Zosim, L.; Chiriac, T.; Bulimaga, V.; Rudic, V.; Turta, C. Biotechnological Application of Homo- and Heterotrinary Iron(III) Furoates for Cultivation of Iron-Enriched Spirulina. *Inorg. Chim. Acta* **2011**, *373*, 167–172. [[CrossRef](#)]
14. Melnic, S.; Prodius, D.; Stoeckli-Evans, H.; Shova, S.; Turta, C. Synthesis and Anti-Tuberculosis Activity of New Hetero(Mn, Co, Ni)Trinary Iron(III) Furoates. *Eur. J. Med. Chem.* **2010**, *45*, 1465–1469. [[CrossRef](#)] [[PubMed](#)]
15. Odularu, A.T.; Ajibade, P.A. Dithiocarbamates: Challenges, Control, and Approaches to Excellent Yield, Characterization, and Their Biological Applications. *Bioinorg. Chem. Appl.* **2019**, *2019*, 8260496. [[CrossRef](#)] [[PubMed](#)]
16. Hogarth, G. Metal-Dithiocarbamate Complexes: Chemistry and Biological Activity. *Mini-Rev. Med. Chem.* **2012**, *12*, 1202–1215. [[CrossRef](#)] [[PubMed](#)]
17. Zhu, L.; Luo, M.; Zhang, Y.; Fang, F.; Li, M.; An, F.; Zhao, D.; Zhang, J. Free Radical as a Double-Edged Sword in Disease: Deriving Strategic Opportunities for Nanotherapeutics. *Coord. Chem. Rev.* **2023**, *475*, 214875. [[CrossRef](#)]
18. Zhang, P.; Sadler, P.J. Redox-Active Metal Complexes for Anticancer Therapy. *Eur. J. Inorg. Chem.* **2017**, *2017*, 1541–1548. [[CrossRef](#)]
19. Kaim, W.; Schwederski, B. Non-Innocent Ligands in Bioinorganic Chemistry—An Overview. *Coord. Chem. Rev.* **2010**, *254*, 1580–1588. [[CrossRef](#)]
20. Kaim, W.; Schwederski, B. Cooperation of Metals with Electroactive Ligands of Biochemical Relevance: Beyond Metalloporphyrins. *Pure Appl. Chem.* **2004**, *76*, 351–364. [[CrossRef](#)]
21. Zhang, T.; Huang, L.Z.; Wu, J.; Lu, D.; Ma, B.L.; Du, Z.T. Microwave-Assisted Synthesis of 2-Substituted 1h-Benzo[d]Imidazoles and Their Antifungal Activities in Vitro. *Heterocycles* **2013**, *87*, 1545–1552. [[CrossRef](#)]
22. Nikiforova, M.E.; Yambulatov, D.S.; Nelyubina, Y.V.; Primakov, P.V.; Bekker, O.B.; Majorov, K.B.; Shmelev, M.A.; Khoroshilov, A.V.; Eremenko, I.L.; Lutsenko, I.A. Current Design of Mixed-Ligand Complexes of Magnesium(II): Synthesis, Crystal Structure, Thermal Properties and Biological Activity against Mycolicobacterium Smegmatis and Bacillus Kochii. *Crystals* **2023**, *13*, 1306. [[CrossRef](#)]
23. Yambulatov, D.S.; Lutsenko, I.A.; Nikolaevskii, S.A.; Petrov, P.A.; Smolyaninov, I.V.; Malyants, I.K.; Shender, V.O.; Kiskin, M.A.; Sidorov, A.A.; Berberova, N.T.; et al. Diimine Cisplatin Derivatives: Synthesis, Structure, Cyclic Voltammetry and Cytotoxicity. *Molecules* **2022**, *27*, 8565. [[CrossRef](#)] [[PubMed](#)]
24. Lutsenko, I.A.; Yambulatov, D.S.; Kiskin, M.A.; Nelyubina, Y.V.; Primakov, P.V.; Bekker, O.B.; Levitskiy, O.A.; Magdesieva, T.V.; Imshennik, V.K.; Maksimov, Y.V.; et al. Improved In Vitro Antimycobacterial Activity of Trinary Complexes Cobalt(II,III) and Iron(III) with 2-Furoic Acid against Mycolicobacterium Smegmatis. *ChemistrySelect* **2020**, *5*, 11837–11842. [[CrossRef](#)]
25. Lutsenko, I.A.; Yambulatov, D.S.; Kiskin, M.A.; Nelyubina, Y.V.; Primakov, P.V.; Bekker, O.B.; Sidorov, A.A.; Eremenko, I.L. Mononuclear Cu(II), Zn(II), and Co(II) Complexes with 2-Furoate Anions and 2,2'-Bpy: Synthesis, Structure, and Biological Activity. *Russ. J. Coord. Chem.* **2020**, *46*, 787–794. [[CrossRef](#)]
26. Yambulatov, D.S.; Nikolaevskii, S.A.; Lutsenko, I.A.; Kiskin, M.A.; Shmelev, M.A.; Bekker, O.B.; Efimov, N.N.; Ugolkova, E.A.; Minin, V.V.; Sidorov, A.A.; et al. Copper(II) Trimethylacetate Complex with Caffeine: Synthesis, Structure, and Biological Activity. *Russ. J. Coord. Chem.* **2020**, *46*, 772–778. [[CrossRef](#)]
27. Potts, K.T. The Chemistry of 1,2,4-Triazoles. *Chem. Rev.* **1961**, *61*, 87–127. [[CrossRef](#)]
28. Council of Europe. *European Pharmacopoeia, 8.0*; European Treaty Series; Council of Europe: Strasbourg, France, 2007; ISBN 9789287160591.
29. Kazeminejad, Z.; Marzi, M.; Shiroudi, A.; Kouhpayeh, S.A.; Farjam, M.; Zarenezhad, E. Novel 1, 2, 4-Triazoles as Antifungal Agents. *Biomed Res. Int.* **2022**, *2022*, 4584846. [[CrossRef](#)] [[PubMed](#)]
30. Paroni, R.; Del Puppo, M.; Borghi, C.; Sirtori, C.R.; Galli Kienle, M. Pharmacokinetics of Ribavirin and Urinary Excretion of the Major Metabolite 1,2,4-Triazole-3-Carboxamide in Normal Volunteers. *Int. J. Clin. Pharmacol. Ther. Toxicol.* **1989**, *27*, 302–307.
31. Amin, N.H.; El-Saadi, M.T.; Ibrahim, A.A.; Abdel-Rahman, H.M. Design, Synthesis and Mechanistic Study of New 1,2,4-Triazole Derivatives as Antimicrobial Agents. *Bioorg. Chem.* **2021**, *111*, 104841. [[CrossRef](#)]
32. Hasegawa, T.; Eiki, J.; Chiba, M. Interindividual Variations in Metabolism and Pharmacokinetics of 3-(6-Methylpyridine-3-Yl-Sulfanyl)-6-(4H-[1,2,4]Triazole-3-Yl-Sulfanyl)-N-(1,3-Thiazole-2-Yl)-2-Pyridine Carboxamide, a Glucokinase Activator, in Rats Caused by the Genetic. *Drug Metab. Dispos.* **2014**, *42*, 1548–1555. [[CrossRef](#)]
33. Sumrra, S.H.; Habiba, U.; Zafar, W.; Imran, M.; Chohan, Z.H. A Review on the Efficacy and Medicinal Applications of Metal-Based Triazole Derivatives. *J. Coord. Chem.* **2020**, *73*, 2838–2877. [[CrossRef](#)]
34. Zafar, W.; Sumrra, S.H.; Chohan, Z.H. A Review: Pharmacological Aspects of Metal Based 1,2,4-Triazole Derived Schiff Bases. *Eur. J. Med. Chem.* **2021**, *222*, 113602. [[CrossRef](#)] [[PubMed](#)]
35. Chohan, Z.H.; Hanif, M. Antibacterial and Antifungal Metal Based Triazole Schiff Bases. *J. Enzyme Inhib. Med. Chem.* **2013**, *28*, 944–953. [[CrossRef](#)] [[PubMed](#)]
36. Hanif, M.; Chohan, Z.H. Design, Spectral Characterization and Biological Studies of Transition Metal(II) Complexes with Triazole Schiff Bases. *Spectrochim. Acta Part A Mol. Biomol. Spectrosc.* **2013**, *104*, 468–476. [[CrossRef](#)] [[PubMed](#)]
37. Chohan, Z.H.; Sumrra, S.H. Some Biologically Active Oxovanadium(IV) Complexes of Triazole Derived Schiff Bases: Their Synthesis, Characterization and Biological Properties. *J. Enzyme Inhib. Med. Chem.* **2010**, *25*, 599–607. [[CrossRef](#)] [[PubMed](#)]

38. Sumrra, S.H.; Hanif, M.; Chohan, Z.H. Design, Synthesis and in Vitro Bactericidal/Fungicidal Screening of Some Vanadyl(IV)Complexes with Mono- and Di-Substituted ONS Donor Triazoles. *J. Enzyme Inhib. Med. Chem.* **2015**, *30*, 800–808. [[CrossRef](#)] [[PubMed](#)]
39. Bormio Nunes, J.H.; Hideki Nakahata, D.; Corbi, P.P.; Ferraz de Paiva, R.E. Beyond Silver Sulfadiazine: A Dive into More than 50 Years of Research and Development on Metal Complexes of Sulfonamides in Medicinal Inorganic Chemistry. *Coord. Chem. Rev.* **2023**, *490*, 215228. [[CrossRef](#)]
40. Bharathi, S.; Mahendiran, D.; Kumar, R.S.; Choi, H.J.; Gajendiran, M.; Kim, K.; Rahiman, A.K. Silver(I) Metallodrugs of Thiosemicarbazones and Naproxen: Biocompatibility, in Vitro Anti-Proliferative Activity and in Silico Interaction Studies with EGFR, VEGFR2 and LOX Receptors. *Toxicol. Res.* **2020**, *9*, 28–44. [[CrossRef](#)]
41. de Souza, C.C.; de Azevedo-França, J.A.; Barrias, E.; Cavalcante, S.C.F.; Vieira, E.G.; Ferreira, A.M.D.C.; de Souza, W.; Navarro, M. Silver and Copper-Benzimidazole Derivatives as Potential Antiparasitic Metallodrugs: Synthesis, Characterization, and Biological Evaluation. *J. Inorg. Biochem.* **2023**, *239*, 112047. [[CrossRef](#)]
42. Raju, S.K.; Karunakaran, A.; Kumar, S.; Sekar, P.; Murugesan, M.; Karthikeyan, M. Silver Complexes as Anticancer Agents: A Perspective Review. *Ger. J. Pharm. Biomater.* **2022**, *1*, 6–28. [[CrossRef](#)]
43. Ji, D.; Wang, Y. An Optimized Protocol of Protargol Staining for Ciliated Protozoa. *J. Eukaryot. Microbiol.* **2018**, *65*, 705–708. [[CrossRef](#)] [[PubMed](#)]
44. Sekito, T.; Sadahira, T.; Watanabe, T.; Maruyama, Y.; Watanabe, T.; Iwata, T.; Wada, K.; Edamura, K.; Araki, M.; Watanabe, M. Medical Uses for Silver Nitrate in the Urinary Tract (Review). *World Acad. Sci. J.* **2022**, *4*, 6. [[CrossRef](#)]
45. Antsiferova, A.A.; Kashkarov, P.K.; Koval'chuk, M.V. Effect of Different Forms of Silver on Biological Objects. *Nanobiotechnol. Rep.* **2022**, *17*, 155–164. [[CrossRef](#)]
46. Suthar, J.K.; Vaidya, A.; Ravindran, S. Toxic Implications of Silver Nanoparticles on the Central Nervous System: A Systematic Literature Review. *J. Appl. Toxicol.* **2023**, *43*, 4–21. [[CrossRef](#)] [[PubMed](#)]
47. McGhie, B.S.; Aldrich-Wright, J.R. Photoactive and Luminescent Transition Metal Complexes as Anticancer Agents: A Guiding Light in the Search for New and Improved Cancer Treatments. *Biomedicines* **2022**, *10*, 578. [[CrossRef](#)]
48. Luengo, A.; Fernández-Moreira, V.; Marzo, I.; Gimeno, M.C. Trackable Metallodrugs Combining Luminescent Re(I) and Bioactive Au(I) Fragments. *Inorg. Chem.* **2017**, *56*, 15159–15170. [[CrossRef](#)]
49. Dasari, S.; Singh, S.; Sivakumar, S.; Patra, A.K. Dual-Sensitized Luminescent Europium(III) and Terbium(III) Complexes as Bioimaging and Light-Responsive Therapeutic Agents. *Chem.—A Eur. J.* **2016**, *22*, 17387–17396. [[CrossRef](#)]
50. Bünzli, J.-C.G. Lanthanide Luminescence for Biomedical Analyses and Imaging. *Chem. Rev.* **2010**, *110*, 2729–2755. [[CrossRef](#)]
51. Visbal, R.; Fernández-Moreira, V.; Marzo, I.; Laguna, A.; Gimeno, M.C. Cytotoxicity and Biodistribution Studies of Luminescent Au(I) and Ag(I) N-Heterocyclic Carbenes. Searching for New Biological Targets. *Dalton Trans.* **2016**, *45*, 15026–15033. [[CrossRef](#)]
52. Ling, Y.; Chen, Z.-X.; Zhou, Y.-M.; Weng, L.-H.; Zhao, D.-Y. A Novel Green Phosphorescent Silver(i) Coordination Polymer with Three-Fold Interpenetrated CdSO<sub>4</sub>-Type Net Generated via in Situ Reaction. *CrystEngComm* **2011**, *13*, 1504–1508. [[CrossRef](#)]
53. Lin, S.; Cui, Y.-Z.; Qiu, Q.-M.; Han, H.-L.; Li, Z.-F.; Liu, M.; Xin, X.-L.; Jin, Q.-H. Synthesis, Characterization, Luminescent Properties of Silver (I) Complexes Based on Organic P-Donor Ligands and Mercaptan Ligands. *Polyhedron* **2017**, *134*, 319–329. [[CrossRef](#)]
54. Pan, J.; Jiang, F.-L.; Wu, M.-Y.; Chen, L.; Gai, Y.-L.; Bawaked, S.M.; Mokhtar, M.; AL-Thabaiti, S.A.; Hong, M.-C. A Series of D10 Metal Clusters Constructed by 2,6-Bis[3-(Pyrazin-2-Yl)-1,2,4-Triazolyl]Pyridine: Crystal Structures and Unusual Luminescences. *Cryst. Growth Des.* **2014**, *14*, 5011–5018. [[CrossRef](#)]
55. Wang, X.; Wang, X.; Jin, S.; Muhammad, N.; Guo, Z. Stimuli-Responsive Therapeutic Metallodrugs. *Chem. Rev.* **2019**, *119*, 1138–1192. [[CrossRef](#)] [[PubMed](#)]
56. Xiong, X.; Liu, L.-Y.; Mao, Z.-W.; Zou, T. Approaches towards Understanding the Mechanism-of-Action of Metallodrugs. *Coord. Chem. Rev.* **2022**, *453*, 214311. [[CrossRef](#)]
57. Stingaci, E.; Zveaghinteva, M.; Pogrebnoi, S.; Lupascu, L.; Valica, V.; Uncu, L.; Smetanscaia, A.; Drumea, M.; Petrou, A.; Ciric, A.; et al. New Vinyl-1,2,4-Triazole Derivatives as Antimicrobial Agents: Synthesis, Biological Evaluation and Molecular Docking Studies. *Bioorg. Med. Chem. Lett.* **2020**, *30*, 127368. [[CrossRef](#)] [[PubMed](#)]
58. Patra, S.A.; Sahu, G.; Das, S.; Dinda, R. Recent Advances in Mitochondria-Localized Luminescent Ruthenium(II) Metallodrugs as Anticancer Agents. *ChemMedChem* **2023**, *18*, e202300397. [[CrossRef](#)] [[PubMed](#)]
59. Bell, R.A.; Kramer, J.R. Structural Chemistry and Geochemistry of Silver-Sulfur Compounds: Critical Review. *Environ. Toxicol. Chem.* **1999**, *18*, 9–22. [[CrossRef](#)]
60. Huang, X.; Li, H.; Tu, Z.; Liu, L.; Wu, X.; Chen, J.; Liang, Y.; Zou, Y.; Yi, Y.; Sun, J.; et al. Highly Conducting Neutral Coordination Polymer with Infinite Two-Dimensional Silver–Sulfur Networks. *J. Am. Chem. Soc.* **2018**, *140*, 15153–15156. [[CrossRef](#)]
61. Silva, R.M.; Smith, M.D.; Gardinier, J.R. Anion- and Solvent-Directed Assembly in Silver Bis(Thioimidazolyl)Methane Chemistry and the Silver–Sulfur Interaction. *Inorg. Chem.* **2006**, *45*, 2132–2142. [[CrossRef](#)]
62. Koshenskova, K.A.; Baravikov, D.E.; Khoroshilov, A.V.; Nelyubina, Y.V.; Primakov, P.V.; Bekker, O.B.; Dokuchaeva, K.S.; Dolgushin, F.M.; Kiskin, M.A.; Eremenko, I.L.; et al. Polymer Cu<sup>2+</sup> and Ag<sup>+</sup> Furancarboxylate Complexes with 4,4'-Bipyridine: Synthetic Approaches, Structure, Thermal Behavior, and Biological Activity. *Russ. Chem. Bull.* **2023**, *72*, 1894–1904. [[CrossRef](#)]

63. Fackler, J.P.; López, C.A.; Staples, R.J.; Wang, S.; Winpenny, R.E.P.; Lattimer, R.P. Self Assembly of Isostructural Copper(I)-Silver(I) Butterfly Clusters with 2-Mercaptothiazoline; Syntheses and Structures of  $(PPh_3)_2Cu_4(C_3H_4NS_2)_4$ ,  $[(C_5H_5N)Cu_4(C_3H_4NS_2)_4]$ ,  $(PPh_3)_2Ag_4(C_3H_4NS_2)_4$  and  $(PPh_3)_2Ag_2Cu_2(C_3H_4NS_2)_4$ . *J. Chem. Soc. Chem. Commun.* **1992**, *2*, 146–148. [[CrossRef](#)]
64. Spek, A. PLATON SQUEEZE: A Tool for the Calculation of the Disordered Solvent Contribution to the Calculated Structure Factors. *Acta Crystallogr. Sect. C* **2015**, *71*, 9–18. [[CrossRef](#)] [[PubMed](#)]
65. Pyykkö, P. Strong Closed-Shell Interactions in Inorganic Chemistry. *Chem. Rev.* **1997**, *97*, 597–636. [[CrossRef](#)] [[PubMed](#)]
66. Schmidbaur, H.; Schier, A. Argentophilic Interactions. *Angew. Chem. Int. Ed.* **2015**, *54*, 746–784. [[CrossRef](#)] [[PubMed](#)]
67. Tsyba, I.; Mui, B.B.; Bau, R.; Noguchi, R.; Nomiya, K. Synthesis and Structure of a Water-Soluble Hexanuclear Silver(I) Nicotinate Cluster Comprised of a “Cyclohexane-Chair”-Type of Framework, Showing Effective Antibacterial and Antifungal Activities: Use of “Sparse Matrix” Techniques for Growing Crystals of Water-Soluble Inorganic Complexes. *Inorg. Chem.* **2003**, *42*, 8028–8032. [[CrossRef](#)] [[PubMed](#)]
68. Whitcomb, D.R.; Swatloski, R.P.; Rogers, R.D. Mode of Complex Formation between Thiones and Silver Ion within a Photothermographic Formulation: The Crystal and Molecular Structure of Hexa(Silver-5-Methyl-2-Mercaptobenzimidazole THF). *J. Imaging Sci. Technol.* **2007**, *51*, 547–551. [[CrossRef](#)]
69. Artem'ev, A.V.; Ryzhikov, M.R.; Berezin, A.S.; Kolesnikov, I.E.; Samsonenko, D.G.; Bagryanskaya, I.Y. Photoluminescence of Ag(I) Complexes with a Square-Planar Coordination Geometry: The First Observation. *Inorg. Chem. Front.* **2019**, *6*, 2855–2864. [[CrossRef](#)]
70. Ramón-García, S.; Ng, C.; Anderson, H.; Chao, J.D.; Zheng, X.; Pfeifer, T.; Av-Gay, Y.; Roberge, M.; Thompson, C.J. Synergistic Drug Combinations for Tuberculosis Therapy Identified by a Novel High-Throughput Screen. *Antimicrob. Agents Chemother.* **2011**, *55*, 3861–3869. [[CrossRef](#)]
71. Bekker, O.B.; Sokolov, D.N.; Luzina, O.A.; Komarova, N.I.; Gatilov, Y.V.; Andreevskaya, S.N.; Smirnova, T.G.; Maslov, D.A.; Chernousova, L.N.; Salakhutdinov, N.F.; et al. Synthesis and Activity of (+)-Usnic Acid and (–)-Usnic Acid Derivatives Containing 1,3-Thiazole Cycle against Mycobacterium Tuberculosis. *Med. Chem. Res.* **2015**, *24*, 2926–2938. [[CrossRef](#)]
72. Lutsenko, I.A.; Baravikov, D.E.; Koshenskova, K.A.; Kiskin, M.A.; Nelyubina, Y.V.; Primakov, P.V.; Voronina, Y.K.; Garaeva, V.V.; Aleshin, D.A.; Aliev, T.M.; et al. What Are the Prospects for Using Complexes of Copper(II) and Zinc(II) to Suppress the Vital Activity of Mycolicibacterium Smegmatis? *RSC Adv.* **2022**, *12*, 5173–5183. [[CrossRef](#)]
73. Polucci, P.; Magnaghi, P.; Angiolini, M.; Asa, D.; Avanzi, N.; Badari, A.; Bertrand, J.; Casale, E.; Cauteruccio, S.; Cirila, A.; et al. Alkylsulfanyl-1,2,4-Triazoles, a New Class of Allosteric Valosine Containing Protein Inhibitors. Synthesis and Structure–Activity Relationships. *J. Med. Chem.* **2013**, *56*, 437–450. [[CrossRef](#)] [[PubMed](#)]
74. Sheldrick, G.M. SHELXT Integrated Space-Group and Crystal-Structure Determination. *Acta Crystallogr. Sect. A* **2015**, *71*, 3–8. [[CrossRef](#)] [[PubMed](#)]
75. Dolomanov, O.V.; Bourhis, L.J.; Gildea, R.J.; Howard, J.A.K.; Puschmann, H. OLEX2: A Complete Structure Solution, Refinement and Analysis Program. *J. Appl. Crystallogr.* **2009**, *42*, 339–341. [[CrossRef](#)]
76. Sheldrick, G.M. A Short History of SHELX. *Acta Crystallogr. Sect. A* **2008**, *64*, 112–122. [[CrossRef](#)]

**Disclaimer/Publisher’s Note:** The statements, opinions and data contained in all publications are solely those of the individual author(s) and contributor(s) and not of MDPI and/or the editor(s). MDPI and/or the editor(s) disclaim responsibility for any injury to people or property resulting from any ideas, methods, instructions or products referred to in the content.